

Removal of o-Cresol from Water by Adsorption/ Photocatalysis

Wojciech Zmudziński*

Department of Commodity Science, Poznań University of Economics,
Al. Niepodległości 10, 61-875 Poznań, Poland

Received: 1 February 2010

Accepted: 24 May 2010

Abstract

This paper presents the results of research on o-cresol adsorption on both C_{active} and $\text{TiO}_2/C_{\text{active}}$, and its photocatalytic oxidation on $\text{TiO}_2/C_{\text{active}}$. It was found that o-cresol adsorption on C_{active} was slow: equilibrium adsorption was reached after more than 20 hours. Adsorption isotherm fulfilled Langmuir equation: $q_{\infty}=1.153 \text{ mmole}\cdot\text{g}^{-1}$, $K=1,324 \text{ dm}^3\cdot\text{mole}^{-1}$. The adsorption was reversible. $\text{TiO}_2/C_{\text{active}}$ as adsorbent behaved similarly to C_{active} itself, although the amount of o-cresol adsorbed per 1 g of $\text{TiO}_2/C_{\text{active}}$ was about 10% smaller. It was concluded, based on the results of two-step experiments, that adsorption and photocatalysis (both the o-cresol dissolved in water and that partly desorbed from the surface of active carbon) was photooxidized when illumination of $\text{TiO}_2/C_{\text{active}}$ followed 26-hour adsorption of the substrate on the photocatalyst-on-adsorbent. The loss of o-cresol dissolved in water fulfilled the 1st order reaction kinetics. It was found in separate experiments that in the presence of illuminated titania, o-cresol molecules underwent hydroxylation preferentially in *para* position vs. original OH group. Hydroxylation of *ortho* position vs. original OH and of the CH_3 group was much slower.

Keywords: photocatalysis, o-cresol, $C_{\text{active}}/\text{TiO}_2$, adsorption, intermediates

Introduction

Billions of tons of industrial waste – gaseous, liquid, and solid – are produced every year all over the world. The waste, especially the liquid ones inhibiting biological functions of all beings, is harmful to the natural environment [1-5]. The broad application of phenolic compounds in many branches of industry, e.g. in production of disinfectants [6], herbicides and pesticides [7], paints, resins, wood preservatives [8-12], tooth fillers [7, 13], and paper and textiles [5, 10, 11, 14, 15] is the reason for their rising concentration in water. For example, liquid waste from the coal pyrolysis process contains $10 \text{ g}\cdot\text{dm}^{-3}$ phenol, catechol, resorcin, xylene, pyrogallol, plus o-, m-, and p-cresols [3, 12]. Cresols are also formed during cigarette smoking, burning

of liquid fuels, wood and coal, and other natural materials [3, 12]. Tiny amounts of p-cresol are produced in nature by some anaerobic bacteria [6, 16].

All phenolics, including cresols, are harmful to both humans and our environment. The compounds are highly stable and soluble in water. Volatile to some extent, they weakly adsorb on soil and tend to be bioaccumulated. Therefore, all methyl derivatives of phenol have been classified by the United States Environmental Protection Agency as stable, priority chemical toxicants [7]. Moreover, because of the proved carcinogenicity their concentration in drinking water should not exceed 10 ppb (USEPA, WHO) [17]. Therefore, appropriate treatment of tap water is necessary in order to lower the contents of phenolics.

Photocatalytic processes on illuminated semiconductors, mainly on TiO_2 , which seemed to be efficient in

*e-mail: w.zmudzinski@ue.poznan.pl

removal of phenol compounds remaining in preliminary purified water, have been extensively studied for the last 30 years [18, 19]. Hydroxyl radicals, the main active species having high oxidation power, are generated on the surface of illuminated TiO_2 ($\lambda \leq 400$ nm). Owing to that photocatalysis on TiO_2 belongs to the so-called AOP's (Advanced Oxidation Processes) [4, 20-22]. In the processes nearly the whole organic matter undergoes full mineralization, i.e. to H_2O and CO_2 . The photocatalytic processes which utilize only active semiconductor and appropriate light (it is possible to utilize sunlight) seem to be the most promising and the cheapest ones among the AOP's. Two crystallographic forms of TiO_2 are recommended as the photocatalyst, anatase, and rutile. Both forms are very stable chemically and photochemically in a broad range of pH, highly active photocatalytically, cheap, and are fully recovered after the process [20, 23-26].

The mechanism of the processes proceeding on TiO_2 the surface is quite well known [27-29]. In short, electrons (e^-) and holes (h^+), photogenerated on the titania surface form active sites, both reductive (e^-) and oxidative (h^+). If their lifetime is sufficiently long, they undergo reactions with solution species. The holes react with water molecules or adsorbed on titania surface OH^- forming hydroxyl radicals. The radicals react further with organic matter oxidizing it (hydroxylation of the compounds have been observed). Excited electrons reduce dissolved oxygen, finally to O^{2-} (some intermediate forms of the reduced oxygen can also have highly oxidative character).

Although the photocatalytic process is fast and relatively efficient, practical application is hindered because of occurrence of titania in a form of fine powder. Attempts have been undertaken in order to immobilize fine titania particles on supports such as SiO_2 , ZrO_2 , C_{active} , polystyrene, glass walls etc. [19, 25, 30-32]. The immobilization causes separation of the solution to be purified from the photocatalyst to be easy. However, some new problems appear: non-stable binding of the photocatalyst to the support, influence of a diffusion process on the overall photocatalytic reaction rate.

In this study fine TiO_2 particles were immobilized on relatively big grains of active carbon, thus allowing easy separation of the photocatalyst from the solution. Removal of o-cresol in the adsorption-photocatalytic process was thoroughly studied in a three phase photoreactor with mobile photocatalyst [33]. Additionally, an effort was undertaken to follow the formation of intermediates of the reaction of o-cresol with photogenerated $\cdot\text{OH}$ radicals.

Experimental

For $\text{TiO}_2/\text{C}_{\text{active}}$ preparation 90 g of active carbon (Sigma, 20-40 mesh) and 10 g TiO_2 (Aldrich, anatase, 99.9%) were mixed in 200 cm^3 of water in a rotating evaporator. Next, the water was evaporated by heating at 100°C. Thus prepared adsorbent/photocatalyst contained about 0.1 g TiO_2 per 1 g $\text{TiO}_2/\text{C}_{\text{active}}$.

TiO_2 particle size was measured with a Mastersizer S (Malvern Instr. Ltd.) automated granulometer using water as a liquid medium. Nitrogen adsorption/desorption isotherm for TiO_2 , C_{active} and the resulting photocatalyst – $\text{TiO}_2/\text{C}_{\text{active}}$, were measured on a Micromeritics automated apparatus. Based on the isotherms, BET-specific surface areas were calculated, as well as surface areas of pores and average pore diameters were estimated from the N_2 adsorption branch following the BJH (Barret-Joyner-Halenda) algorithm.

Both adsorption and photocatalytic experiments were carried out in an air lift loop photoreactor (ca 200 cm^3 volume) described elsewhere [21, 33, 34]. Initial o-cresol (Aldrich, 99%) concentrations in water were: $1 \cdot 10^{-3}$, $9 \cdot 10^{-4}$, $8 \cdot 10^{-4}$, $7 \cdot 10^{-4}$, and $6 \cdot 10^{-4}$ mole \cdot dm $^{-3}$, both in adsorption and photocatalytic experiments. The reactor contained 165 cm^3 of o-cresol solution. During the experiments 0.5 cm^3 samples of the solution were withdrawn from the reactor at appropriate time intervals, and filtered on Millipore Millex GV $_3$ units. O-cresol concentration was analyzed on a Varian 2800 gas chromatograph equipped with FID detector and 3 m glass column (1 mm diameter) filled with 0.1% Alltech AT-1000 on Graphpac (80-100 mesh), and maintained at 200°C.

Adsorption experiments were carried out using either 0.09 g C_{active} or 0.1 g $\text{TiO}_2/\text{C}_{\text{active}}$; time of the experiments was 26 hours. During the experiments the reactor was kept in darkness, at room temperature ($20 \pm 1^\circ\text{C}$) and under argon atmosphere. The reactor contents were mixed by a stream of argon (3.0 dm $^3 \cdot$ h $^{-1}$).

Photocatalytic experiments consisted of two steps:

1. adsorption of o-cresol in darkness, under argon atmosphere (26 hours), and
2. photooxidation of the compound in air under UV-visible irradiation.

The reactor was illuminated from the side by a light of 180W medium pressure Hg lamp and cooled by an air stream. Reaction temperature was maintained at $28 \pm 1^\circ\text{C}$. Reactor content was mixed using streams of argon (adsorption) or air (photocatalysis).

To determine the intermediates of o-cresol photocatalytic oxidation, 0.01 g TiO_2 (anatase, 99.9%, Aldrich) was added to 165 ml of $6 \cdot 10^{-4}$ mole \cdot dm $^{-3}$ o-cresol solution and sonicated for 5 min. Then the slurry was poured to the reactor and a photocatalytic reaction was conducted in the way described above. During illumination 1 ml of the slurry was withdrawn at appropriate time intervals using a syringe and, after filtration over Millipore Millex GV $_3$ units, analyzed by HPLC (Waters) using a photodiode array detector (Waters 991). The reaction products were separated on a Supelcosil LC8 column using water-methanol with a gradient concentration as an eluent. o-Cresol, methylhydroquinone, 3-methylcatechol, and 2-hydroxybenzylalcohol were identified from their retention times and UV spectra. Quantitative determinations were done based on calibration curves.

The water used for the adsorption and photocatalytic studies was doubly distilled in a quartz water still. All reactants were of *p.a.* purity or HPLC specified ones.

Table 1. BET-specific surface area, BJH adsorption surface area of pores, BJH adsorption average pore diameter and pore volume of TiO₂, C_{active}, and TiO₂/C_{active}.

Sample	BET surface area	Pore surface area	Average pore diameter	Pore volume
	m ² ·g ⁻¹	m ² ·g ⁻¹	Å	cm ³ ·g ⁻¹
TiO ₂	11.9	11.9	136	0.04
C _{active}	604	218	53	0.29
TiO ₂ /C _{active}	478	180	53	0.24

Results and Discussion

The photocatalyst, TiO₂/C_{active} is composed of two substances that possess different properties: large adsorption capacity (C_{active}), and high photocatalytic activity (TiO₂/C_{active}). The TiO₂/C_{active} grains, prepared in a simple way, remained stable during nearly thirty-hour experiments; TiO₂ did not come off the photocatalyst-on-adsorbent particles. It should be added here that titania itself forms a very fine powder with an average particle size of about 0.1 μm (89% of the particles have diameters in the range of 0.07-0.2 μm). The simple preparation method was chosen intentionally: in this way the activity of both TiO₂ (photocatalytic activity) and C_{active} (the adsorption one) was preserved, although somewhat reduced. Table 1 shows textural properties of the substrates – TiO₂ and C_{active}, and of the resulting photocatalyst/adsorbent – TiO₂/C_{active}.

The data in Table 1 show that binding of the low surface area photocatalyst, TiO₂, onto the high surface area adsorbent, C_{active}, causes about 20% reduction of the surface area of the active carbon. At the same time about 18% of the pores of C_{active} were blocked by the fine TiO₂ particles.

As mentioned above, the first part of the paper is devoted to *o*-cresol adsorption on active carbon and on TiO₂/C_{active}. It was found in preliminary experiments that *o*-cresol was not adsorbed on TiO₂ in a measurable amount. Therefore, it seemed to be justified to present the results of adsorption experiments on C_{active} itself. Some comparisons of the adsorption of *o*-cresol on C_{active} and TiO₂/C_{active} were also made. The adsorption experiments were conducted using 0.09 g C_{active} and 0.1 g TiO₂/C_{active}. Note, however, that in both cases the amount of C_{active} were the same, 0.09 g, thus allowing a simple comparison of adsorption properties of both samples.

The results of *o*-cresol adsorption on active carbon using various concentrations of the adsorbate are shown in Fig. 1. It should be added here that whereas the time necessary to reach adsorption equilibrium was about 20 hours for C_{active}, it was somewhat shorter for TiO₂/C_{active} and was about 17 hours.

At least two conclusions can be drawn from the data in Fig. 1:

1. adsorption is a slow process, and
2. the amount of *o*-cresol adsorbed at equilibrium depends on its initial concentration.

A plot of *o*-cresol adsorbed vs. initial *o*-cresol concentration is shown in Fig. 2, both for C_{active} and TiO₂/C_{active}.

It is evident from the data in Fig. 2 that adsorption of *o*-cresol on TiO₂/C_{active} is slightly lower, by about 10%, than on active carbon itself. Note, that 1 g of TiO₂/C_{active} contains 0.9 g active carbon. In both cases the dependence of the amount of *o*-cresol adsorbed at equilibrium (per 1 g of the adsorbent) on initial adsorbate concentration is linear. This means, according to the adsorption theory, that the adsorption is reversible. The reversibility of adsorption was con-

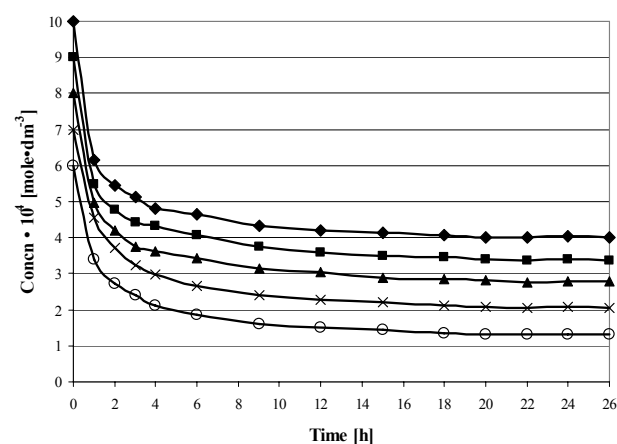


Fig. 1. *o*-Cresol adsorption on active carbon at various concentrations of the adsorbate. Conditions: liquid volume, 165 ml; *o*-cresol conc. 6.0-10.0·10⁻⁴ mole·dm⁻³; C_{active} weight, 0.09 g; temp. 20±1°C.

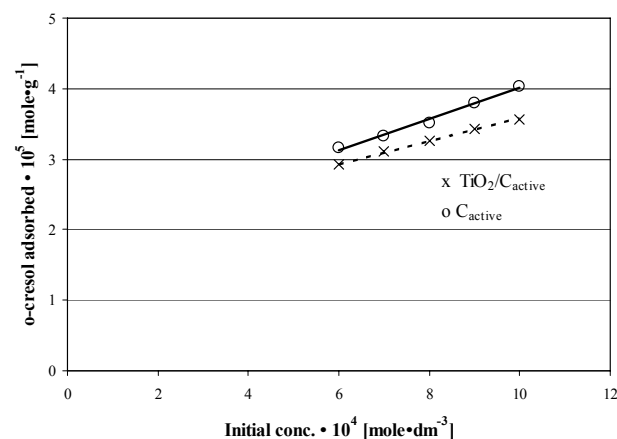


Fig. 2. Adsorption isotherms of *o*-cresol on active carbon and TiO₂/C_{active}.

Table 2. Amount of o-cresol adsorbed at equilibrium on C_{active} and $\text{TiO}_2/C_{\text{active}}$ at different concentrations of the adsorbate. C_{active} weight, 0.09 g; $\text{TiO}_2/C_{\text{active}}$ weight, 0.1 g; temp. $20 \pm 1^\circ\text{C}$.

Initial o-cresol conc. mole·dm ⁻³ ·10 ⁴	Amount of o-cresol adsorbed			
	C_{active}		$\text{TiO}_2/C_{\text{active}}$	
	mole·g ⁻¹ ·10 ³	mole·m ⁻² ·10 ⁵	mole·g ⁻¹ ·10 ³	mole·m ⁻² ·10 ⁵
10	10.9	1.80	9.7	2.03
9	10.3	1.70	9.2	1.92
8	9.6	1.59	8.9	1.86
7	9.0	1.49	8.5	1.78
6	8.6	1.42	7.9	1.65

firmed experimentally. After 26-hour adsorption of o-cresol on C_{active} , the solution was removed and the reactor filled up with 165 cm³ of pure water. Next, o-cresol concentration was determined again during 24 hours. The results are shown in Fig. 3. It is evident that concentration of o-cresol in the added water increases slowly.

Adsorption of o-cresol on active carbon fulfils the Langmuir equation, which in a linear form is as follows:

$$\frac{c_{eq}}{q_{eq}} = \frac{c_{eq}}{q_{\infty}} + \frac{1}{Kq_{\infty}}$$

...where: q_{∞} , maximum amount of adsorbate per 1 g (or 1 m²) of adsorbent; q_{eq} , amount of adsorbate adsorbed at its equilibrium concentration c_{eq} on 1 g (or 1 m²) of the adsorbent; K , a constant of adsorption equilibrium.

A plot of c_{eq}/q_{eq} vs. c_{eq} is shown in Fig. 4. The linear dependence confirms that adsorption of o-cresol on active carbon fulfils the Langmuir equation. Calculated Langmuir constants for o-cresol adsorption on active carbon are as follows: $q_{\infty}=1.153 \text{ mole} \cdot \text{g}^{-1}$, $K=1,324 \text{ dm}^3 \cdot \text{mole}^{-1}$.

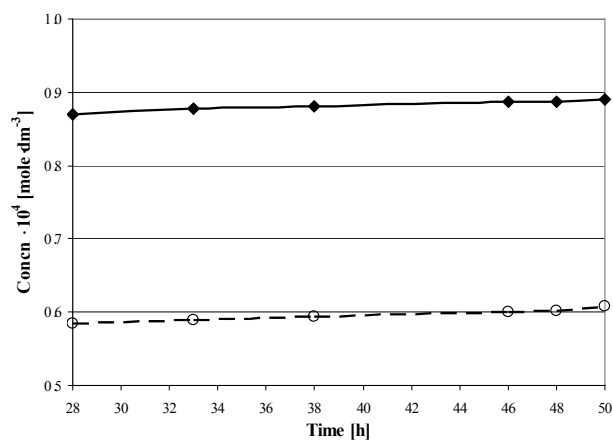


Fig. 3. Desorption of o-cresol from C_{active} . Conditions: liquid volume, 165 ml; o-cresol conc. 8.0 and $10.0 \cdot 10^4 \text{ mole} \cdot \text{dm}^{-3}$; C_{active} weight, 0.09 g; temp. $20 \pm 1^\circ\text{C}$. The substrate was adsorbed for 26 hours, and then the solution was removed and the reactor filled again with pure water.

The amounts of o-cresol adsorbed at equilibrium on C_{active} and $\text{TiO}_2/C_{\text{active}}$ are shown in Table 2.

Taking into account that specific surface area of $\text{TiO}_2/C_{\text{active}}$ is smaller than that of C_{active} , the decrease of the amount of o-cresol adsorbed per 1 g of the samples is not surprising. However, the amount of the adsorbate per 1 m² is higher for $\text{TiO}_2/C_{\text{active}}$, on average of 16%. It is concluded therefore that the part of pores of active carbon is not accessible for o-cresol adsorption. These pores are probably blocked by the bound titania particles diminishing, thus adsorption of N_2 utilized for surface area measurements and, consequently, reducing surface area (calculated from the data of N_2 adsorption experiments).

Two-step experiments were designed for studying photocatalytic activity of $\text{TiO}_2/C_{\text{active}}$. The first reaction step, o-cresol pre-adsorption, proceeding mainly on the photocatalyst support, active carbon, was conducted in darkness, under argon atmosphere, in order to prevent any substrate oxidation. After the adsorption equilibrium had been established (i.e. after 17-hour dark adsorption), the mixture was aerated and illumination started. It should be added here that the amount of the catalyst (0.10 g) and space velocity of the gas (argon or air), were well chosen experimentally. Initial o-cresol concentration was 6, 7, 8, 9, and $10 \cdot 10^4 \text{ mole} \cdot \text{dm}^{-3}$.

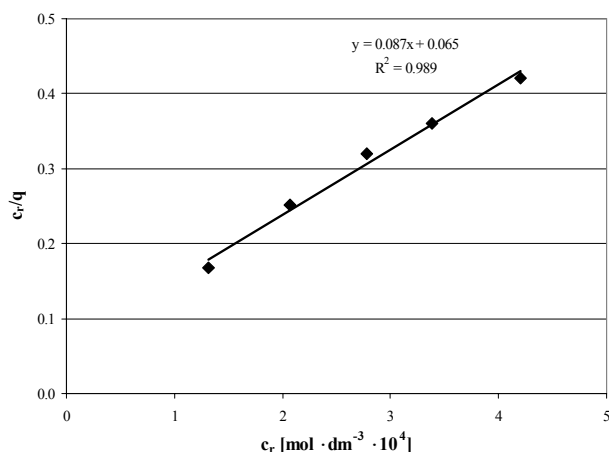


Fig. 4. A plot of c_{eq}/q_{eq} vs. c_{eq} .

Fig. 5 shows, as an example, the course of the whole process for the highest *o*-cresol concentration, $10.0 \cdot 10^{-4}$ mole dm^{-3} . Both steps of the reaction likewise the adsorption equilibrium are well seen on Fig. 5. The photocatalyst support, active carbon, removes large amount of *o*-cresol from the solution by simple adsorption. Further water purification proceeds via photocatalytic reaction on TiO_2 surface. It is expected that also a part of previously adsorbed *o*-cresol is oxidized during the photocatalytic reaction; see the discussion below.

Fig. 6 shows the decrease of *o*-cresol concentration in the solution during illumination of $\text{TiO}_2/\text{C}_{\text{active}}$. The photocatalytic experiments were run after the equilibrium adsorption had been established, i.e. after about 60% (for the highest initial *o*-cresol concn.) to 80% (for the lowest *o*-cresol concn.) of the substrate had been removed from the solution by simple adsorption, see Fig. 1.

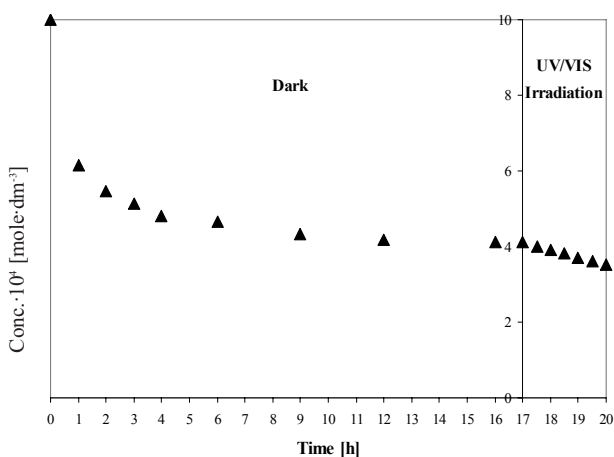


Fig. 5. Adsorption – photocatalysis two step experiment. *o*-Cresol initial concentration, $10.0 \cdot 10^{-4}$ mole dm^{-3} . Conditions: liquid volume, 165 ml; $\text{TiO}_2/\text{C}_{\text{active}}$ weight, 0.1 g; 180 W Hg medium pressure lamp; adsorption temp. $20 \pm 1^\circ\text{C}$; reaction temp. $28 \pm 1^\circ\text{C}$.

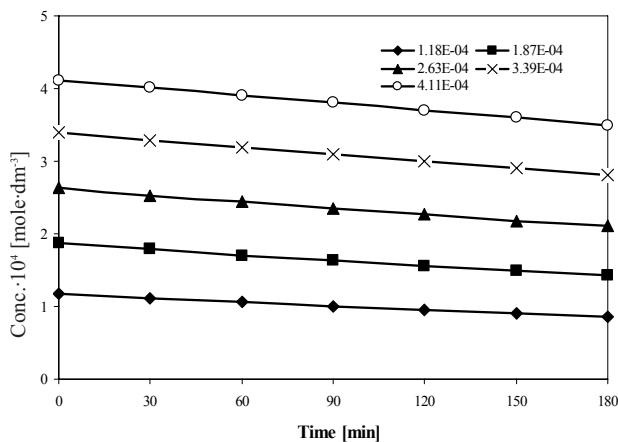


Fig. 6. Kinetic curves of *o*-cresol decay in the solution during illumination of $\text{TiO}_2/\text{C}_{\text{active}}$. Conditions: liquid volume, 165 ml; *o*-cresol initial conc. 6.0; 7.0; 8.0; 9.0, and $10.0 \cdot 10^{-4}$ mole dm^{-3} ; $\text{TiO}_2/\text{C}_{\text{active}}$ weight, 0.1 g; temp. $28 \pm 1^\circ\text{C}$; 180 W Hg medium pressure lamp. Individual curves refer to different *o*-cresol concentration.

Photocatalytic reactions of any chemical compound destruction can be described by a kinetic expression. A full kinetic equation, which included such parameters as substrate concentration, amount of a photocatalyst, air pressure and light intensity, has been given by Okamoto et al. [35]. In the case described here all reaction parameters, except *o*-cresol concentration, were kept constants. Therefore, the kinetic equation would comprise only one variable, substrate concentration. According to the abounding subject literature, see e.g. [36] and refs. therein, photocatalytic reactions obey 1st order kinetic rule. Moreover, Langmuir-Hinshelwood mechanism is usually recommended, i.e. the reaction proceeds between surface $\cdot\text{OH}$ radicals, generated by light, and adsorbed surface molecules. The resultant Langmuir-Hinshelwood equation in a linear form is given below.

$$\frac{1}{r} = \frac{1}{k} + \frac{1}{k \cdot K_{\text{ads}}} \cdot \frac{1}{c}$$

...where: c is the substrate concentration in water, k a rate constant, and K_{ads} the constant of adsorption equilibrium.

Therefore, if *o*-cresol photocatalytic oxidation obeys 1st order kinetic, the plot of reciprocal of the reaction rate vs. reciprocal of substrate concentration should be linear. The plot of $1/r$ vs. $1/c$ is depicted in Fig. 7.

In this case $r = dc/dt$ means the initial reaction rate, c – initial *o*-cresol concentration, i.e. the equilibrium concentration of the substrate after its adsorption on active carbon (catalyst support). The dependence of $1/r$ vs. $1/c$ is linear, with a correlation factor being 0.95. It should be mentioned here that the initial reaction rates are related only to *o*-cresol. With time many intermediates of the photocatalytic reactions are formed. They compete with the main substrate for hydroxyl radicals reducing the rate of *o*-cresol photooxidation. Some of the intermediates were identified and quantitatively determined, see below.

It was proved, see above, that *o*-cresol adsorbed reversibly on active carbon. Therefore, it can be supposed, that during the photoreaction desorption of *o*-cresol follows the decrease of its concentration in the liquid phase enhancing it. Hence true amount of reacted *o*-cresol can be expected.

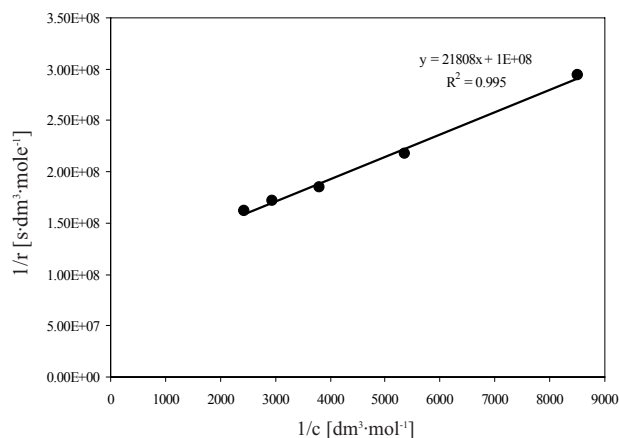


Fig. 7. A plot of $1/r$ vs. $1/c$.

ed to be somewhat higher than that calculated from the data of Fig. 7. Moreover, the proximity of the desorbed substrate particles to active sites on titania should enhance their oxidation. In this study active carbon, which plays the role of a photocatalyst support, removes a large amount of o-cresol from the solution (60 to 80%, as mentioned above) by simple adsorption. However, it seems that the active carbon also enhances the reaction rate owing to the desorption of the substrate closed to the sites at which $\cdot\text{OH}$ radicals are photogenerated.

As mentioned in *Experimental*, the photocatalytic experiments for intermediate determination were performed using 165 ml of $6 \cdot 10^{-4}$ mole \cdot dm $^{-3}$ o-cresol solution and 0.01 g of pure TiO $_2$ as the photocatalyst. Results of the photocatalytic experiments are shown in Figs. 8A and 8B.

Only three among five possible hydroxylated derivatives were detected and quantitatively determined, namely methylhydroquinone, 3-methylcatechol and 2-hydroxybenzylalcohol, based on their retention times and spectra. The results confirmed that photooxidation on illuminated TiO $_2$ occurred *via* generation of $\cdot\text{OH}$ radicals and a reaction of

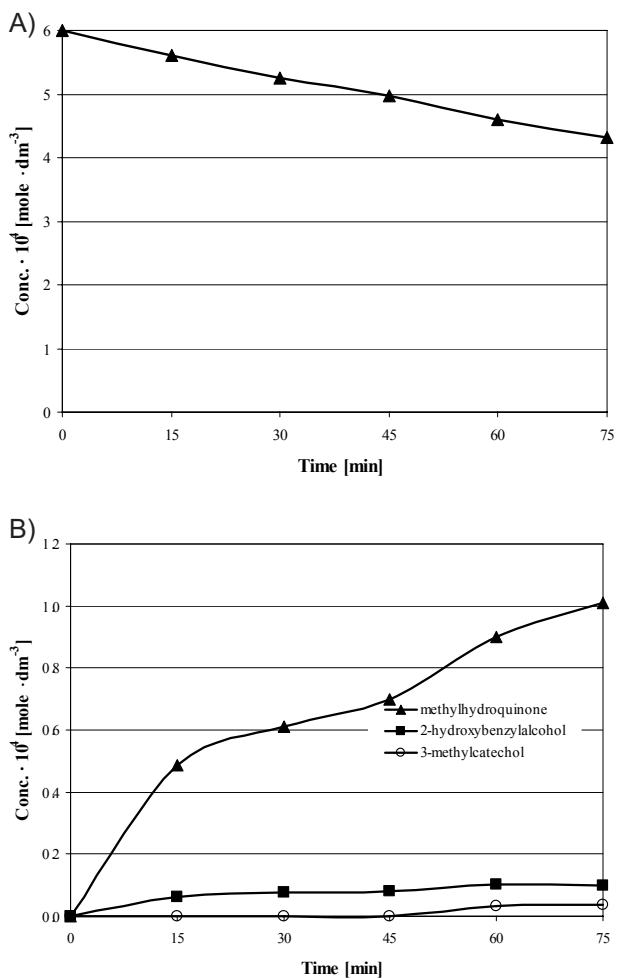


Fig. 8. A) A kinetic curve of o-cresol delay versus time on illuminated TiO $_2$. B) Variations of intermediate concentration during illumination of $6 \cdot 10^{-4}$ mole \cdot dm $^{-3}$ o-cresol solution. Conditions: liquid volume, 165 ml; o-cresol initial conc. $6.0 \cdot 10^{-4}$ mole \cdot dm $^{-3}$; TiO $_2$ weight, 0.01 g; temp. $28 \pm 1^\circ\text{C}$; 180 W Hg medium pressure lamp.

the radicals with organic compounds. In the case of o-cresol the $\cdot\text{OH}$ radicals are preferentially bound at *para* position vs. original hydroxyl group. Hydroxylation of the methyl group was about ten times slower, and bounding of $\cdot\text{OH}$ into *ortho* position was even three times slower than the methyl group hydroxylation. It should be added here that relatively fast hydroxylation of phenol at *para* position and much slower at the *ortho* one was reported before in one of the previous articles from this laboratory [34].

Summary and Conclusions

A combination of adsorption and photocatalysis was applied in order to remove o-cresol, a dangerous pollutant, from water. It was found, that o-cresol adsorption on C_{active} was slow: although during the first two hours about 50% of o-cresol was removed from water, equilibrium adsorption was reached after about 20 hours. The adsorption fulfilled the Langmuir equation of adsorption isotherm: maximal o-cresol adsorption $q_{\text{e}} = 1.153$ mmole \cdot g $^{-3}$, and constant of adsorption equilibrium $K = 1,324$ dm 3 \cdot mole $^{-1}$. It was established experimentally that the adsorption was reversible. o-Cresol adsorption on TiO $_2$ / C_{active} was found to proceed similarly to that on C_{active} itself, the amount of the substrate adsorbed per 1 g of TiO $_2$ / C_{active} was about 10% lower. The results of two-step experiments – adsorption and photocatalysis – led to the conclusion that both the o-cresol dissolved in water and that desorbed from the surface of active carbon was photooxidized when illumination of TiO $_2$ / C_{active} followed overnight adsorption of the substrate on the photocatalyst-on-adsorbent. Under the conditions, the loss of o-cresol dissolved in water fulfilled the 1st order reaction kinetics. It was also found that o-cresol molecules underwent hydroxylation in the presence of illuminated titania, preferentially in *para* position vs. original OH group. Hydroxylation of *ortho* position vs. original OH and of CH $_3$ group was much slower.

References

1. FAISAL M., TARIQ M., MUNEER M. Photocatalysed degradation of two selected dyes in UV-irradiated aqueous suspensions of titania, *Dyes Pigm.* **72**, 233, **2007**.
2. ARUTHELVAN V., KANAKASABAI V., ELANGO VAN R., NAGARAJAN S., MURALIKRISHNAN V. Kinetics of high strength phenol degradation using *Bacillus Brevis*, *J. Hazard. Mater.* **B129**, 216, **2006**.
3. FLOX C., CABOT P-L., CENTELLAS F., GARRIDO J.A., RODRIGUEZ R.M., ARIAS C., BRILLAS E. Solar photo-electro-Fenton degradation of cresols using a flow reactor with a boron-doped diamond anode, *Appl. Catal. B: Environm.* **75**, 17, **2007**.
4. KAVITHA V., PALANIVELU K. The role of ferrus ion in Fenton and photo-Fenton processes for the degradation of phenol, *Chemosphere* **55**, 1235, **2004**.
5. RAJKUMAR D., PALANIVELU K. Electrochemical treatment of industrial wastewater, *J. Hazard. Mat.* **B113**, 123, **2004**.

6. SINGH R.K., KUMAR S., KUMAR S., KUMAR A. Biodegradation kinetic studies for the removal of *p*-cresol from wastewater using *Glomastix indicus* MTCC 3869, *Biochem. Eng. J.* **40**, 293, **2008**.
7. KAVITHA V., PALANIVELU K. Destruction of cresols by Fenton oxidation process, *Water Res.* **39**, 3062, **2005**.
8. TSAI S-Y., JUANG R-S. Biodegradation of phenol and sodium salicylate mixtures by suspended *Pseudomonas putida* CCRC 14365, *J. Hazard. Mat.* **B138**, 125, **2006**.
9. BAI J., WEN J-P., LI H-M., JIANG Y., Kinetic modeling of growth and biodegradation of phenol and *m*-cresol using *Alcaligenes faecalis*, *Proc. Biochem.* **42**, 510, **2007**.
10. GODJEVARGOVA T., IVANOVA D., ALEKSIEVA Z., BURDELOVA G. Biodegradation of phenol by immobilized *Trichosporon cutaneum* R57 on modified polymer membranes, *Proc. Biochem.* **41**, 2342, **2006**.
11. MAEDA M., ITOH A., KAWASE Y. Kinetics for aerobic biological treatment of *o*-cresol containing wastewaters in a slurry bioreactor: biodegradation by utilizing waste activated sludge, *Biochem. Eng. J.* **22**, 97, **2005**.
12. SANTOS A., YUSTOS P., RODRIGUEZ S., GARCIA-OCHOA F. Wet oxidation of phenol, cresols and nitrophenols catalyzed by activated carbon in acid and basic media, *Appl. Catal. B: Environm.* **65**, 269, **2006**.
13. CALDERON-GUZMAN D., HERNANDEZ-ISLAS J.L., VAZQUEZ I.R.E., BARRAGAN-MEJIA G., HERNANDEZ-GARCIA E., ANGEL D.S., JUAREZ-OLGUIN H. Effect of toluene and cresols on Na⁺, K⁺-ATPase, and serotonin in rat brain, *Reg. Toxicol. Pharmacol.* **41**, 1, **2005**.
14. SARAVANAN P., PAKSHIRAJAN K., SAHA P. Biodegradation of phenol and *m*-cresol in a batch and fed batch operated internal loop airlift bioreactor by indigenous mixed microbial culture predominantly *Pseudomonas* sp., *Biores.Technol.* **99**, 8553, **2008**.
15. SARAVANAN P., PAKSHIRAJAN K., SAHA P. Batch growth kinetics of an indigenous mixed microbial culture utilizing *m*-cresol as the sole carbon source, *J. Hazard. Mat.* **162**, 476, **2009**.
16. SANDERS J.M., BUCHER J.R., PECKHAM J.C., KISSLING G.E., HEJTMANCIK M.R., CHHABRA R.S. Carcinogenesis studies of cresols in rats and mice, *Toxicology* **257**, 33, **2009**.
17. NUHOGLU A., YALCIN B., Modelling of phenol removal in a batch reactor, *Proc. Biochem.* **40**, 1233, **2005**.
18. CHEN H-W., KU Y., KUO Y-L. Effect of Pt/TiO₂ characteristic on temporal behavior of *o*-cresol decomposition by visible light-induced photocatalysis, *Water Res.* **41**, 2069, **2007**.
19. KUO Y-L., CHEN H-W., KU Y. Analysis of silver particles incorporated on TiO₂ coatings for the photodecomposition of *o*-cresol, *Thin Solid Films* **515**, 3461, **2007**.
20. ZIELIŃSKA B., GRZECHULSKA J., KALEŃCZUK R., MORAWSKI A.W. The pH influence on photocatalytic decomposition of organic dyes over A11 and P25 titanium dioxide, *Appl.Catal.B: Environm.* **45**, 293, **2003**.
21. DOBOSZ A., SOBCZYŃSKI A. The influence of silver additives on titania photoactivity in the photooxidation of phenol, *Water Res.* **37**, 1489, **2003**.
22. KAVITHA V., PALANIVELU K. Degradation of nitrophenols by Fenton and photo-Fenton processes, *J. Photochem Photobiol. A: Chem* **170**, 83, **2005**.
23. SUN L., LU H., ZHOU J. Degradation of H-acid by combined photocatalysis and ozonation processes, *Dyes Pigm.* **76**, 604, **2008**.
24. MANSILLA H., MORA A., PINCHEIRA C., MONDACA M., MARCATO P. DURAN N., FREER J., New photocatalytic reactor with TiO₂ coating on sintered glass cylinders, *Appl. Catal. B: Environm.* **76**, 57, **2007**.
25. MILLS J., LEPRE A., ELLIOTT N., BHOPAL S., PARKIN I., O'NEILL S. Characterisation of the photocatalyst Pilkington Activ™: a reference film photocatalyst? *J. Photochem. Photobiol. A: Chem.* **160**, 213, **2003**.
26. ZOU L., LUO Y., HOOPER M., HU E. Removal of VOCs by photocatalysis process using adsorption enhanced TiO₂-SiO₂ catalyst, *Chem. Eng. Process.* **45**, 959, **2006**.
27. HATIPOGLU A., SAN N., CINAR Z. An experimental and theoretical investigation of the photocatalytic degradation of *meta*-cresol in TiO₂ suspensions: a model for the product distribution, *J. Photochem. Photobiol. A: Chem.* **165**, 119, **2004**.
28. CARPIO E., ZUNIGA P., PONCE S., SOLIS J., RODRIGUEZ J., ESTRADA W. Photocatalytic degradation of phenol using TiO₂ nanocrystals supported on activated carbon, *J. Mol. Catal. A: Chem.* **228**, 293, **2005**.
29. TARIQ M., FAISAL M., SAQUIB M., MUNEEB M. Heterogeneous photocatalytic degradation of an anthraquinone and a triphenylmethane dye derivative in aqueous suspensions of semiconductor, *Dyes Pigm.* **76**, 358, **2008**.
30. ARABATZIS I.M., STERGIPOPOULOS T., ANDREEVA D., KITOVA S., NEOPHYTIDES S., FALARAS P. Characterization and photocatalytic activity of Au/TiO₂ thin films for azo-dye degradation, *J. Catal.* **220**, 127, **2003**.
31. JANUS M., TRYBA B., INAGAKI M., MORAWSKI A.W. New preparation of a carbon-TiO₂ photocatalyst by carbonization of *n*-hexane deposited on TiO₂, *Appl. Catal. B: Environm.* **52**, 61, **2004**.
32. TRYBA B., MORAWSKI A.W., INAGAKI M. A new route for preparation of TiO₂-mounted activated carbon, *Appl. Catal. B: Environm.* **46**, 203, **2003**.
33. SOBCZYŃSKI A., JIMENES J., CERVERA-MARCH S., Photodecomposition of phenol in a flow reactor: adsorption and kinetics, *Monatsch.Chem.* **128**, 1109, **1997**.
34. SOBCZYŃSKI A., DUCZMAL Ł., ZMUDZIŃSKI W. Phenol destruction by photocatalysis on TiO₂: an attempt to solve the reaction mechanism, *J. Mol. Catal. A: Chem.* **213**, 225, **2004**.
35. OKAMOTO K., YAMAMOTO Y., TANAKA H., ITAYA A. Heterogeneous Photocatalytic Decomposition of Phenol over TiO₂ Powder, *Bull. Chem. Soc. Jpn.* **58**, 1985, **1985**.
36. SOBCZYŃSKI A., DOBOSZ A. Water Purification by Photocatalysis on Semiconductors, *Pol. J. Environ. Stud.* **10**, 195, **2001**.

